

Article

Anticorrosive Effects of Essential Oils Obtained from White Wormwood and Arâr Plants

Ghada Beniaich¹, Mustapha Beniken¹, Rajae Salim¹, Nadia Arrousse¹ , Elhachmia Ech-chihbi¹ , Zakia Rais¹ , Asmae Sadiq², Hiba-Allah Nafidi³, Yousef A. Bin Jordan⁴ , Mohammed Bourhia^{5,*}  and Mustapha Taleb¹

- ¹ Laboratory of Engineering, Electrochemistry, Modeling and Environment, Faculty of Sciences, Sidi Mohamed Ben Abdellah University, Fez 30050, Morocco; ghadabeniaich@gmail.com (G.B.)
- ² Laboratory of Engineering and Materials LIMAT, Faculty of Sciences Ben M'Sik, Department of Physics, Hassan II University, Casablanca 7955, Morocco
- ³ Department of Food Science, Faculty of Agricultural and Food Sciences, Laval University, Quebec City, QC G1V 0A6, Canada
- ⁴ Department of Pharmaceutics, College of Pharmacy, King Saud University, Riyadh P.O. Box 11451, Saudi Arabia
- ⁵ Department of Chemistry and Biochemistry, Faculty of Medicine and Pharmacy, Ibn Zohr University, Laayoune 70000, Morocco
- * Correspondence: bourhiamohammed@gmail.com

Abstract: This article is part of the contribution to the development of two medicinal plants widely used by the Moroccan population: white wormwood (*Artemisia herba-alba*) and Arâr (*Juniperus phoenicea*), species belonging to the Asteraceae and Cupressaceae families, respectively. The present work was conducted to investigate the chemical composition and anticorrosive properties of essential oils (EOs) extracted from these plants. The chemical analysis of the essential oils (EOs) was carried out by GC-MS/MS. Potentiodynamic polarization, electrochemical impedance spectroscopy (EIS), and quantum chemical calculations by density-functional theory at B3LYP were used to study the anticorrosive effect of the researched oils on mild steel in 1 M hydrochloric acid solution. Moreover, SEM-EDX analysis was used to identify the surface morphology of mild steel surface. GC-MSMS results showed the presence of 32 potentially active compounds in the EOs of *Artemisia herba-alba*. The average yield of the EOs was about 1.39 ± 0.17 mL/100 g dry matter. Beta thujone (30.07%) and alpha thujone (13.32%) are the main components, while for the EOs of *Juniperus phoenicea*, the study showed the presence of 30 constituents, with alpha-pinene (43.61%) and manoyl oxide (11.5%) as the main components. The average yield of HE was 1.10 ± 0.03 mL/100 g dry matter. The findings demonstrated an important anticorrosive action of EOs from *Artemisia herba-alba* and *Juniperus phoenicea*. Notably, the experimental results showed good efficiency of the studied essential oils and correlated well with the density-functional theory (DFT) calculations. The results of potentiodynamic polarization measurements showed that hydrazone acted as a mixed-type inhibitor. The EIS results showed an increase in charge transfer resistance accompanied by a noticeable decrease in C_{dl} values, revealing that both studied oils were effective as reliable inhibitors for the protection of mild steel in 1 M HCl solution. Also, the efficiency decreased with decreasing inhibitor concentrations. Surface studies ensure the effectiveness of both investigated oils and the reduction of the surface roughness of mild steel. Furthermore, DFT results of the major constituents of *Artemisia herba-alba* and *Juniperus phoenicea* EOs revealed insights into the chemical reactivity of the tested oils while supporting the experimental conclusions and showed outstanding adsorption ability of both investigated EOs on the steel surface.

Keywords: aromatic plants; *Artemisia herba-alba*; *Juniperus phoenicea*; essential oil; anticorrosive activity; potentiodynamic polarization; impedance spectroscopy



Citation: Beniaich, G.; Beniken, M.; Salim, R.; Arrousse, N.; Ech-chihbi, E.; Rais, Z.; Sadiq, A.; Nafidi, H.-A.; Bin Jordan, Y.A.; Bourhia, M.; et al. Anticorrosive Effects of Essential Oils Obtained from White Wormwood and Arâr Plants. *Separations* **2023**, *10*, 396. <https://doi.org/10.3390/separations10070396>

Academic Editor: Ahmed Mohamed Abd-ElGawad

Received: 29 April 2023

Revised: 22 June 2023

Accepted: 26 June 2023

Published: 10 July 2023



Copyright: © 2023 by the authors. Licensee MDPI, Basel, Switzerland. This article is an open access article distributed under the terms and conditions of the Creative Commons Attribution (CC BY) license (<https://creativecommons.org/licenses/by/4.0/>).

1. Introduction

Morocco has a very rich botanical heritage, but due to a lack of knowledge of the potential wealth it can bring, it is unfortunately rarely used. Nature has plants that serve as food for animals and humans [1,2]. Man has discovered many other functions that plants can provide, and currently, aromatic plants are a promising source of essential oils with a wide range of applications in health care, cosmetology, agriculture, food, and corrosion inhibitors [3]. Plants represent a huge source of bioactive molecules exploited in industry, namely corrosion inhibitors, which are used to protect the material from deterioration due to its interaction (chemical or electrochemical) with the environment. Corrosion is a costly problem for the chemical industry. Furthermore, it is very costly and has a major impact on the economy of industrialized countries [4]. Corrosion not only has economic implications, but it also poses risks to human life and safety. It represents a public danger by causing serious accidents and thus contributes significantly to environmental pollution [4]. Several available methods can be used to slow down or prevent corrosion of metal structures [5]. However, the use of a corrosion inhibitor is generally the most economical, attractive, effective, and acceptable way to reduce the rate of corrosion and protect metal surfaces from corrosion [6]. Acid pickling, industrial acid cleaning, acid descaling, and oil well acidification are the main applications. These organic substances are either synthetically created or derived from medicinal and culinary plants. Biological and environmental factors have supported their use as corrosion inhibitors. Many plant components have been shown to be very effective corrosion inhibitors for iron and steel in acidic environments, according to previous studies [7,8].

The genus *Artemisia*, which includes 500 species spread across Europe, North America, Asia, and South Africa, is commonly present in the Mediterranean region [8]. *Artemisia herba-alba* is a low, green, and woody shrub. Due to its morphological and physiological properties, it is well adapted to dry climatic conditions. It can reduce water loss from transpiration by using the seasonal dimorphism of its foliage. Because of its large root system, *Artemisia herba-alba* can take advantage of the slightest precipitation [9]. The essential oils (EOs) produced by several species of this genus are well-known and used in the culinary, cosmetic, and pharmaceutical sectors [9,10]. There are 14 species of *Artemisia* in Morocco, eight of which are native to Morocco [11,12]. *Artemisia* essential oils have demonstrated biological effects, including antibacterial, antioxidant, anti-inflammatory, insecticidal, and anticorrosive activity [13,14].

Juniperus phoenicea belongs to the family Cupressaceae, which consists of about 130–140 species. It is abandoned in the Canary Islands and North Africa (Algeria, Morocco, and Tunisia) [15–17]. *Juniperus* is classified into three sections: Caryocedrus, Oxycedrus, and Sabina [15]. It is a tree or shrub five to ten meters tall, with evergreen, thin, linear, prickly, needle-like leaves. Its flowers produce fleshy, globular fruits that are mistakenly called berries. *Juniperus* grows wild in dry, rocky, drought-prone terrain. *Juniperus phoenicea* essential oil has many pharmacological effects, including antibacterial, anti-inflammatory, antiviral, expectorant, sedative, herbicidal, insect-repellent, and odorant properties [16].

In the present work, the chemical composition, and the anticorrosive properties of the essential oils of *Artemisia herba-alba* and *Juniperus phoenicea* were studied in depth.

2. Materials and Methods

2.1. Plant Material

Juniperus phoenicea was collected in Tirnes (33°29'47" N; 3°48'36" W), while *Artemisia herba-alba* was collected in Tighboula (32°36'36" N; 6°00'36" W) in Morocco during May 2019 (Figure 1). A botanist at the University Sidi Mohamed Ben Abdellah University carried out the botanical identification wherein the reference specimen number BD01/11281 was given to *Juniperus phoenicea* and the reference specimen number BA23/13010 was given to *Artemisia herba-alba*. The harvested plants were dried in the shade in open air for three days.



Figure 1. *Juniperus phoenicea* (A); *Artemisia herba-alba* (B).

2.2. Extraction of Essential Oils

Briefly, 100 g of *Juniperus phoenicea* and *Artemisia herba-alba* leaves were used for extraction by use of hydrodistillation. Next, anhydrous sodium sulfate was used to dry the EOs before storing them in a refrigerator at 4 °C until further use [18]. The essential oil yield, expressed as a percentage, was estimated by calculating the ratio between the volume of EO and the mass of plant material used according to the following formula:

$$R (\%) = \frac{VHE}{MV} \times 100$$

where R: yield of essential oil (%); VHE: volume of essential oil (mL); MV: mass of plant material (g).

2.3. EO Chemical Analysis (GC-MS)

The chemical makeup of the EOs was investigated using a triple quadrupole, tandem mass spectrometer and gas chromatograph TQ8040 NX (Shimadzu, Tokyo, Japan) (GC-MSMS). The EO chemical compounds were identified using an apolar, capillary RTxi-5 Sil MS column (30.00 m long, 0.25 mm inside diameter, and film thickness of 0.25 µm). The temperatures at the source and interface were 200 °C and 280 °C, respectively. Helium was used as the carrier gas (with an injection volume of 1 µL). The oven temperature was programmed to rise from 50 °C to 160 °C for 2 min at a rate of 5 °C/min, then to 280 °C for 2 min at a rate of 5 °C/min. The injection mode was split with a split opening at 4 min, temperature of 250 °C, and pressure of 37.10 kPa. A percentage of the total peak area was used to represent the EO composition. EO components were identified by comparing the resulting retention indices with those of the literature database [18].

2.4. Anti-Corrosion Activity

2.4.1. Electrochemical Analysis

The electrochemical experiment was performed using a potentiostat of type Versa-STAT 4 controlled with the Versa-Studio analysis program. This method was performed in a three-electrode glass cell. The used specimen served as the working electrode, while a platinum wire served as the counter electrode and an Ag/AgCl/KCl saturated reference electrode. The sample, a square with a 1 cm² exposed surface, was also ground with 1500 grit grinding papers, cleaned with distilled water, degreased with acetone, and then submerged in the destructive test solution (1.0 M hydrochloric acid [HCl] solution made from 37% analytical reagent grade HCl by dilution with double-distilled water with and without inhibitors) for 30 min until the open circuit potential was reached. Impedance tests were recorded in the frequency range 100 kHz–100 mHz. In addition, polarization curves were plotted at a sweep rate of 1 mV/s [19].

2.4.2. Theoretical Calculation

Density-Functional Theory (DFT) to Define B3LYP

In the presence of water molecules, the DFT approach was used at B3LYP with the 6-311G/(d,p) basis set and the Gaussian 09 program [20]. The highest energy molecular orbital energy (E_{HOMO}) and lowest energy orbital that has the scope to accept electron energy (E_{LUMO}), as well as other features, are among the quantum descriptors that were retrieved in the output file [21]:

$$\Delta E_{gap} = E_{LUMO} - E_{HOMO}$$

$$\chi = \frac{1}{2}(E_{HOMO} + E_{LUMO})$$

$$\eta = \frac{1}{2}(E_{LUMO} - E_{HOMO})$$

$$\sigma = \frac{1}{\eta}$$

Also, using the following Equation (2), the fraction of electrons transmitted by the inhibitor to the surface of steel (110) (N110) was computed [21]:

$$\Delta N(110) = \frac{\chi_{metal} - \chi_{inh}}{2(\eta_{metal} + \eta_{inh})}$$

Surface Analysis

After six hours of immersion in 1 M HCl solutions, both with and without inhibitors at a concentration of 1 g/L, mild steel samples were examined using SEM-EDX spectroscopy to determine their surface composition and morphology [22]. The study was carried out using a model QUANTA 200 environmental scanning electron microscope with an EDX probe connected to energy dispersive spectroscopy (EDX) at a 15 kV accelerating voltage.

3. Results and Discussion

3.1. Chemical Composition of *Artemisia herba-alba* and *Juniperus phoenicea* EOs

3.1.1. Essential Oils from *Artemisia herba-alba*

The average yield of EO extracted from *Artemisia herba-alba* was $1.39 \pm 0.17\%$ of the total mass of dry matter. This percentage is similar to that of EO extracted from *A. herba-alba* collected in Jordan (1.3%) [23], and higher than that of *A. herba-alba* collected in southern Morocco at 1.2% [24]. The average yield of *A. herba-alba* EO collected in Guercif ranged from 0.56% to 1.23% [25], and that of the plant collected in Matmata in Tunisia was 0.65% [9]. On the other hand, the average yield of *A. herba-alba* EO collected in Spain ranged from 0.56% to 1.23% [25], and that of the plant grown in Biskra and M'sila in Algeria was 0.95% and 1.02%, respectively [26,27]. The present study identified 32 constituents of *Artemisia herba-alba* EOs (Table 1). In this study, beta-thujone (30.07%) and alpha-thujone (13.32%) were identified as the main constituents of EOs, followed by a few compounds such as spirojatamol (2.95%), sabinene (0.75%), terpinen-4-ol (2.09%), globulol (2.95%), 1,8-cineole (4.67%), endo-borneol (0.64%), thymol (0.71%), beta-santalol (3.38%), and caryophyllene oxide (0.93%). These results are consistent with the chemical composition of *A. herba-alba* EOs grown in Mediterranean regions [28,29]. However, some chemicals present in the *Artemisia herba-alba* EOs studied in the present study have been noted for *A. herba-alba* growing in other regions [30,31].

3.1.2. Essential Oils from *Juniperus phoenicea*

The average yield of EOs extracted from *Juniperus phoenicea* was $1.10 \pm 0.03\%$ dry matter. This rate is lower than that found in southern Tunisia, at 2.004% [32]. It is quite comparable to the EO from the same plant harvested in central-western Tunisia (1%) [33],

and higher than that of red juniper in other regions of Morocco: 0.98% for Assif Almal, 0.90% for Mehdiya [34]; 0.5% for Oujda Angade [35], and 0.9% for Marrakech [36].

Table 1. Constituents of essential oils from *Artemisia herba-alba* and *Juniperus phoenicea*.

Peaks	Retention Time	Kovats Index		Compounds	Area (%)	
		Literature	Calculated		<i>A. herba-alba</i>	<i>J. phoenicea</i>
1	3.435	737	733	Norbornene	0.70%	-
2	7.989	939	939	alpha-Pinene	-	43.61%
3	8.999	930	925	Thujene	1.41%	-
4	9.138	975	976	Sabinene	0.75%	-
5	10.433	1024	1024	p-Cymene	0.70%	-
6	10.661	979	979	p-Menthane, 1,8-epoxy	2.53%	-
8	10.761	1014	1014	p-Cineole	2.10%	-
9	10.906	1031	1032	1,8-Cineole	4.67%	-
10	12.593	1096	1095	Linalool	-	0.83%
11	12.904	1096	1092	Linalool	-	2.88%
12	12.949	1138	1140	Thujanone	0.84%	-
13	13.152	1102	1102	Isothujone	13.12%	-
14	13.310	1102	1004	Alpha-thujone	13.32%	0.82%
15	13.550	1114	1114	Beta-thujone	30.07%	-
16	13.961	1141	1141	cis-Verbenol	-	0.68%
17	14.105	1142	1142	cis-Sabinol	0.75%	-
18	14.177	1141	1141	2-Pinen-4-ol, trans-	-	1.04%
19	14.312	1144	1144	trans-Verbenol	-	3.16%
20	15.068	1169	1169	endo-Borneol	0.64%	-
21	15.315	1177	1174	Terpinen-4-ol	2.09%	-
22	15.750	1195	1196	Myrtenal	-	1.37%
23	16.093	1205	1205	Verbenone	-	1.52%
24	17.441	1363	1363	cis-4-Decenol	-	0.68%
25	18.580	1290	1290	Thymol	0.71%	-
26	20.833	1260	1262	Benzyl propanoate	-	1.22%
27	21.128	1390	1390	beta-Elementene	-	1.18%
28	21.955	1408	1410	Caryophyllene	-	2.01%
29	22.152	1561	1561	Germacrene B	-	1.18%
30	22.906	1288	1290	Bornyl acetate	0.76%	-
31	23.040	1137	1135	cis-p-Mentha-2,8-dienol	0.69%	-
32	23.205	1485	1488	Germacrene D	0.80%	-
33	23.824	1290	1290	Sabinyl acetate	1.01%	-
34	24.183	1689	1688	Shyobunol	-	0.82%
35	24.866	1017	1017	geranyl-.alpha.-terpinene	-	1.55%
36	25.022	1578	1574	Spathulenol	-	1.08%
37	25.171	1549	1544	Elemol	-	2.31%
38	25.855	1602	1602	Ledol	0.63%	2.55%

Table 1. Cont.

Peaks	Retention Time	Kovats Index		Compounds	Area (%)	
		Literature	Calculated		<i>A. herba-alba</i>	<i>J. phoenicea</i>
39	26.024	1578	1576	Spathulenol	1.08%	1.22%
40	26.200	1583	1583	Caryophyllene oxide	0.93%	4.34%
41	26.881	1590	1592	Globulol	1.93%	-
42	27.025	1648	1644	Agarospirol	2.95%	-
43	27.339	1640	1640	Alpha Cadinol	0.96%	-
44	27.526	1630	1630	Iso-spathulenol	4.45%	-
45	27.596	1338	1332	Gamma-Elemene	4.45%	-
46	27.738	1900	1900	Columellarin	1.89%	-
47	28.242	1658	1655	Bisabolol oxide B	1.13%	-
48	28.465	1675	1675	alpha-Santalol	0.78%	-
49	29.816	2206	2202	Isospathulenol	-	0.83%
50	29.973	1702	1702	beta-Santalol	3.38%	-
51	30.704	1685	1680	alpha-Bisabololoxide A	0.92%	-
52	31.253	1460	1458	Allo-aromadendrene oxide	-	1.83%
53	31.598	1490	1490	6-Eudesmen-4- α -ol	1.15%	-
54	32.286	1466	1466	Caryophyllene epoxide	-	1.41%
55	32.410	1600	1662	Rosifoliol	-	0.61%
56	32.605	1490	1485	beta-Selinene	-	0.63%
57	32.685	1607	1603	beta-Oplophenone	-	0.96%
58	36.392	2216	2214	Manool oxide	-	11.50%
59	40.151	2468	2468	Abictol	-	0.94%
60	43.429	1032	1030	Hexanedioic acid	-	4.41%

On the other hand, the average yield of *Juniperus phoenicea* EO was between 0.50% and 0.75% in Tunisia [9,37], 0.36% in Egypt [38], 0.41% in Portugal, 0.21% in Greece, and 0.30% and 0.70% in Spain [39].

The present study identified 30 constituents for *Juniperus phoenicea* EOs (Table 1). In this study, alpha-pinene (43.61%) and manoyl oxide (11.50%) were identified as the main constituents of EO [40,41], followed by a few compounds such as linalol (2.88%), thujone (0.82%), trans-verbenol (3.16%), spathulenol (0.83%), allo-aromadrene oxide (1.83%), geranyl-alphaterpinene (1.55%), verbenone (1.52%), and germacrene B (1.18%). Based on previous research, our results are in agreement with the chemical composition of *Juniperus phoenicea* collected in several regions, as reported in previous works [33–41].

3.2. Anticorrosion Activity

Figure 2 depicts the polarization curves obtained for mild steel in acidic environments in the absence and presence of various HE inhibitor concentrations. Table 2 shows the electrochemical parameters, including the current densities, corrosion potential, and the cathodic slope (β_c). Numerous studies have classified the different types of inhibitors based on the difference in corrosion potential between the inhibited electrolyte solution and the control. The type of inhibitor (anodic or cathodic) is determined by whether or not the E_{corr} value is greater than or less than 85 mV [42]. The obtained results showed that the examined EOs are classified as mixed-type inhibitors because the change in E_{corr} value was less than 85 mV. Table 2 shows that the i_{corr} current densities decrease as the concentrations of *Artemisia herba-alba* and *Juniperus phoenicea* inhibitors increase. This indicates an increase

in the inhibition efficiency of the EOs. Our findings demonstrate that the synergistic interaction of diverse organic compounds in the two EOs led to the production of protective layers on the mild steel surface. Indeed, corrosion inhibition was tested for natural extracts by several researchers, and their results proved very promising and eco-friendly [43]. At the optimal concentration, the efficiency of the studied EOS was 92% for *Juniperus phoenicea* inhibitor and 91% for *Artemisia herba-alba* inhibitor in our study. Also, we can observe the effectiveness of the studied inhibitor at low concentrations, notably the efficiency at 0.25 g/L for both EOs at about 80%, which may favor the use of these EOs to fight against corrosion of mild steel in molar hydrochloric solution [44].

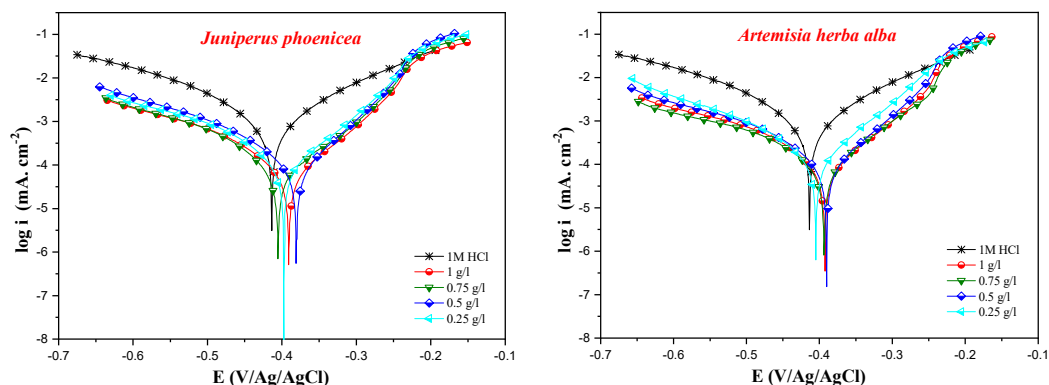


Figure 2. Polarization curves of mild steel in 1 M HCl in the presence of various concentrations of the *Juniperus phoenicea* and *Artemisia herba-alba* inhibitors.

Table 2. Potentiodynamic polarization parameters of mild steel in HCl solution with the addition of *Artemisia herba-alba* and *Juniperus phoenicea* EOs at 298 °K.

	Conc (g/L)	$-E_{corr}$ (mV/Ag/AgCl)	i_{corr} ($\mu A\ cm^{-2}$)	β_c (mV dec ⁻¹)	η_{PDP} (%)
1 M HCl	**	413	944	139	00
<i>Juniperus phoenicea</i>	1	391	75	108	92
	0.75	405	87	104	91
	0.5	381	97	107	90
	0.25	396	105	102	89
<i>Artemisia herba-alba</i>	1.00	392	81	138	91
	0.75	394	96	135	90
	0.50	389	105	130	89
	0.25	404	162	128	83

** : no inhibition percentage for the blank solution.

The impedance investigation was conducted to better comprehend the inhibition mechanism and the mild steel’s ability to guard against corrosion in an aggressive environment and the presence of two inhibitors with plant origin. Figure 3 displays the two inhibitors and their respective impedance plots in the Nyquist plane. In Table 3, the impedance parameters are categorized. The following equation was used to calculate the inhibitory efficiency:

$$\eta_{imp} \% = \frac{R_{ct} - R'_{ct}}{R_{ct}} \times 100$$

where R_{ct} and R'_{ct} are the charge transfer resistance in the presence and absence of inhibitors, respectively.

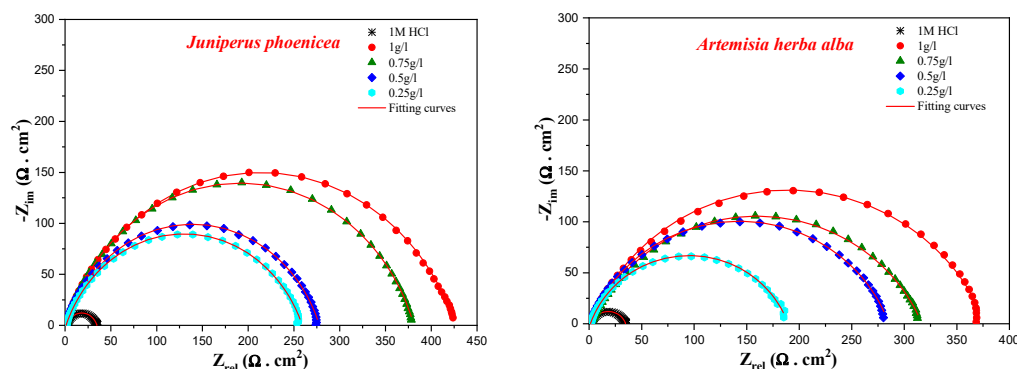


Figure 3. Impedance diagrams in the Nyquist plots of mild steel obtained in 1 M HCl in the presence of different concentrations of *Artemisia herba-alba* and *Juniperus phoenicea* inhibitors.

Table 3. Impedance parameters of mild steel in 1 M HCl containing different concentrations of the studied EOs.

	Conc. (g/L)	R_s ($\Omega \text{ cm}^2$)	R_{ct} ($\Omega \text{ cm}^2$)	C_{dl} ($\mu\text{F} \cdot \text{cm}^{-2}$)	n_{dl}	Q ($\mu\text{F} \cdot \text{S} \cdot \text{cm}^{-1}$)	η_{imp} %
1 M HCl	**	1.76	33.2	89.10	0.784	312.7	00
<i>Juniperus phoenicea</i>	1	0.94	425.4	32.78	0.781	83.23	92
	0.75	1.06	379.9	41.03	0.806	91.76	91
	0.5	0.53	277.2	46.80	0.791	116.1	88
	0.25	1.04	258.0	53.79	0.773	141.6	87
<i>Artemisia herba-alba</i>	1	1.7	375.3	31.6	0.777	85	91
	0.75	2.2	314.7	31.9	0.753	99	89
	0.5	0.9	284.4	43.7	0.784	113	88
	0.25	1.2	188.2	51.2	0.787	137	82

** : no inhibition percentage for the blank solution.

Due to surface heterogeneity, the diagrams from Nyquist plots have imperfect half loops, which suggests that the inhibition mechanism of the corrosion process is controlled by the charge transfer process [45]. Moreover, the diameter of the capacitive loop grows as the concentration of the tested inhibitors increases. From the electrochemical parameters (Table 3 and Figure 4), the values of polarization resistance R_p rise with increasing inhibitor concentration, showing an improvement in the examined inhibitors' efficacy, to reach a maximum value of 92% for the two EOs under study at a concentration of 1 g/L. This could be explained by the formation of an inhibitor film on the surface of the working electrode. Parallel to this, a decline in the CDL double layer's capacity was seen as a result of the gradual adsorption of inhibitor molecules in place of water molecules [46].

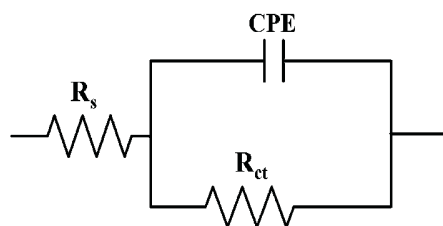


Figure 4. The suitable equivalent circuit used to fit EIS data.

Investigating the connection between an inhibitor's structure and its electrical and corrosion properties is achievable theoretically (Table 4). Moreover, Figures 5 and 6 display the electron density and electrostatic charge of electrons (ESPMs) distribution between

the elements of the HOMO and LUMO atomic orbits. This finding indicates that the examined EOs' electron molecules share a common metal-d route because the majority of their reaction space is dispersed correctly, as seen by the HOMO and LUMO orbitals. Also, according to the ESPMM classification, oxygen atoms determine the overall density of red pigments in molecular electrostatic potential (MEP) analysis. This can lead to adsorption effects on mild steel [47]. For *Artemisia herba-alba* EOs, the responsible compounds send electrons to the mild steel surface because of the higher value of E_{HOMO} as compared to other molecules. In addition, beta-santalole has the smallest energy gap, which can explain the anti-corrosion properties of beta-santol more than those of thujone and eucalyptol molecules [48]. For *Juniperus phoenicea* EOs, the pinene component shares electrons with the d-vacant orbital of iron more than other molecules [49]. In addition, caryophyllene oxide has a small energy gap that reflects its reactivity compared to other products [47]. According to Lukovist's study [45], enhancing the metal's ability to donate electrons can slow the corrosion process because all investigated molecules have a ΔN value of <3.6 [46]. When it comes to the value of the dipole moment, some authors claim that corrosion prevention rises with effectiveness, while others claim that it is inconsistent and therefore useless. Our measurements are able to evaluate the effectiveness of various molecules in the studied EOs [49].

Table 4. Theoretical parameters for *Artemisia herba-alba* and *Juniperus phoenicea* inhibitors in the aqueous phase.

EOs	Descriptors	E_{HOMO} (eV)	E_{LUMO} (eV)	ΔE_{gap} (eV)	η (eV)	σ (eV ⁻¹)	χ (eV)	ΔN (eV)
<i>Artemisia herba-alba</i>	Thujone	-6.860	-0.829	6.031	3.015	0.331	3.845	0.161
	Eucalyptol	-6.601	0.873	7.474	3.737	0.267	2.863	0.261
	Beta-santalol	-6.428	-0.909	5.519	2.759	0.362	3.668	0.208
<i>Juniperus phoenicea</i>	Pinene	-6.1964	0.4729	6.6693	3.3346	0.2998	2.8617	0.2936
	Manoyl oxide	-6.7698	0.1404	6.9102	3.4551	0.2894	3.3146	0.2178
	Hexanedioicacid	-7.7058	0.0897	7.7956	3.8978	0.2565	3.8080	0.1298
	Caryophylleneoxide	-6.6356	0.0059	6.6416	3.3208	0.3011	3.3148	0.2266

Figure 7 shows the morphological properties of mild steel after 6 h of immersion in 1 M hydrochloric acid, both with and without the optimum concentration of *Juniperus phoenicea* and *Artemisia herba-alba* (1 g/L). The resulting EDX spectra are shown in Figure 8 along with a breakdown of the various atomic element adsorption rates on the mild steel surface in Table 5.

Table 5. Percentage of atomic elements obtained by EDX spectra.

Element	<i>Juniperus phoenicea</i>	<i>Artemisia herba-alba</i>	Blank
C	7.94	7.36	0.30
O	6.61	6.02	7.53
Si	0.24	0.44	0.00
Cr	0.35	0.29	0.25
Mn	0.83	0.79	0.60
Fe	84.02	85.09	77.16

As a result of the attack of the aggressive solution (1 M HCl alone) in the absence of inhibitors, the mild steel surface was highly damaged and heavily corroded, due to the rapid rate of iron dissolving in a corrosive environment. However, after adding 1 g/L of *Juniperus phoenicea* and *Artemisia herba-alba* to the acidic solution, the surface became more

uniform and smoother [50]. Compared to the blank, the surface of the material treated with inhibitors was protected. These results confirm the ability of the two studied EOs to prevent surface corrosion of mild steel in 1 M HCl solution by creating a layer of surface coating that grants protection against corrosion.

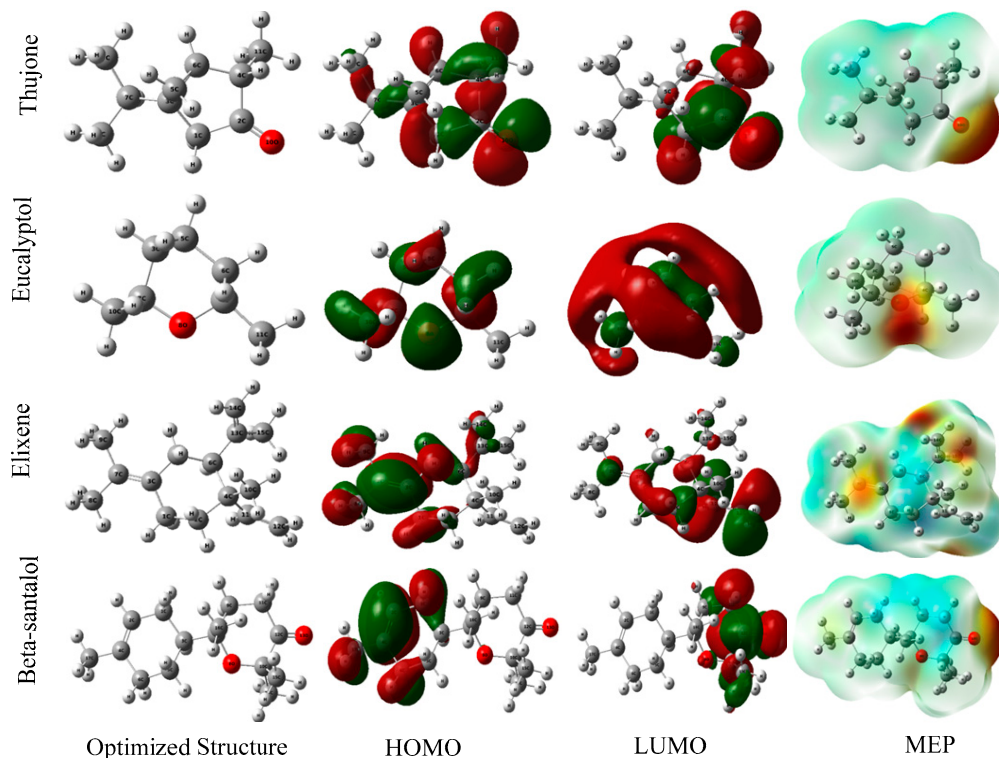


Figure 5. Spatial distributions of *Artemisia herba-alba* inhibitors in the aqueous phase.

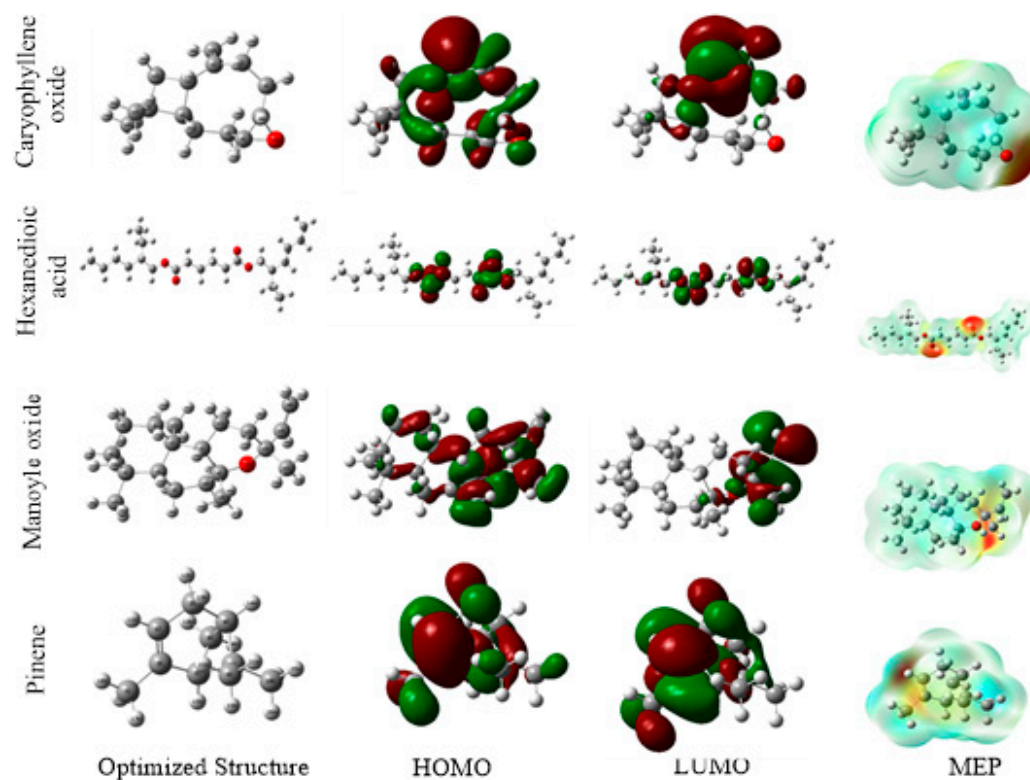


Figure 6. Spatial distributions of *Juniperus phoenicea* inhibitors in the aqueous phase.

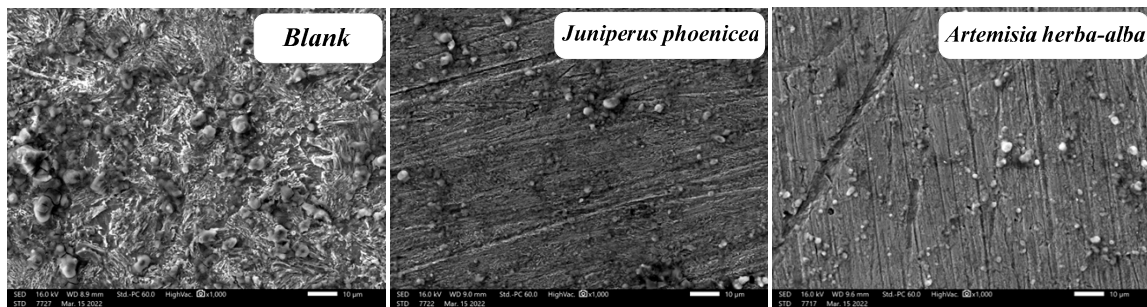


Figure 7. SEM images of mild steel after 6 h of immersion in 1 M HCl solution and in the presence of *Artemisia herba-alba* and *Juniperus phoenicea* inhibitors.

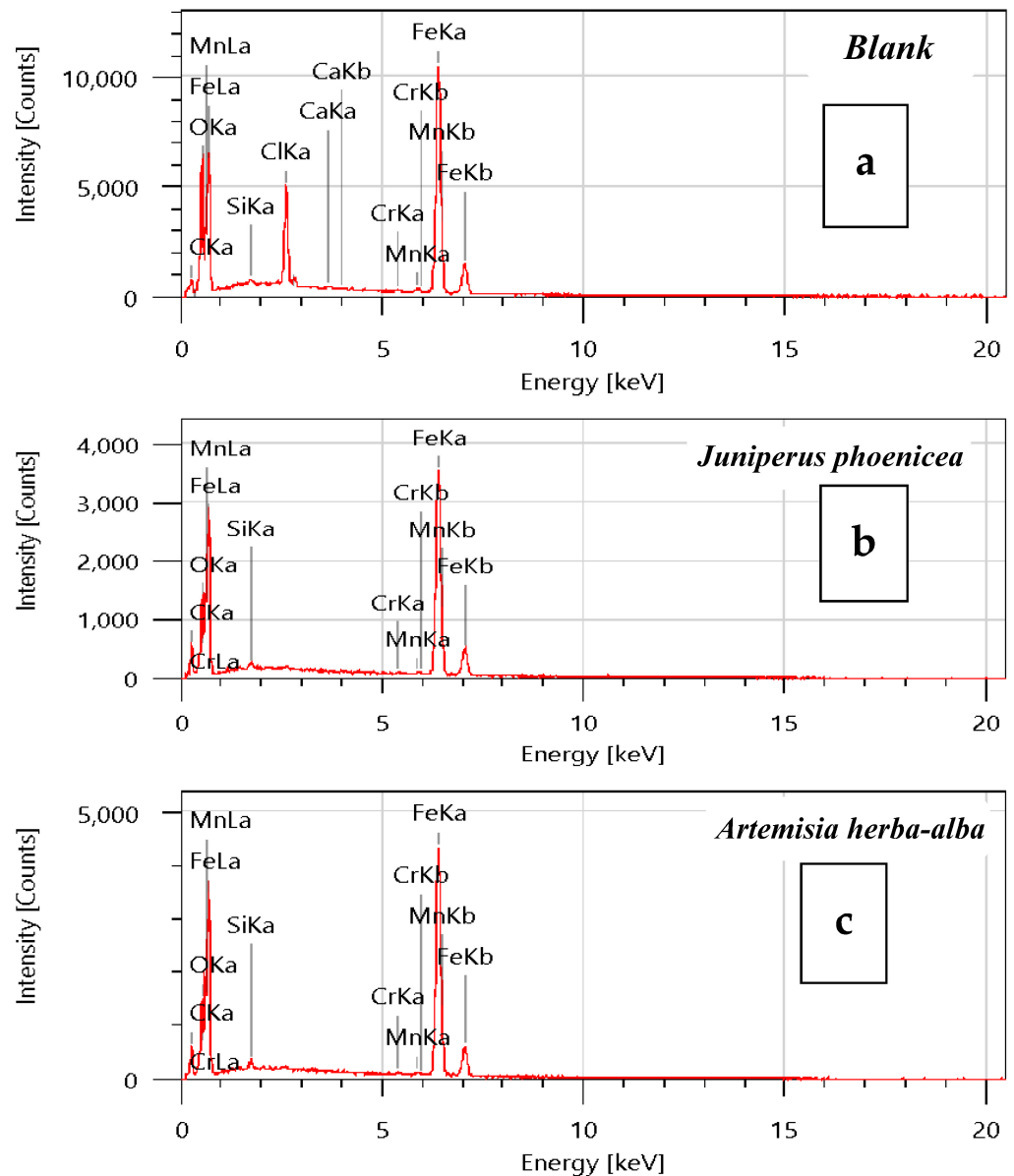


Figure 8. EDX spectra of mild steel after 6 h immersion in 1 M HCl solution (a) and in the presence of *Juniperus phoenicea* (b) *Artemisia herba-alba* (c).

On the other hand, EDX was used to determine the initial composition of mild steel samples before and after the addition of the examined inhibitors. The increase in carbon atom percentages in EOs is visible in the EDX spectra. When the *Juniperus phoenicea*

inhibitor is present, the amount of carbon atoms increases, which can be explained by the components of the investigated EOs adhering to the surface and forming a protective layer [51]. Moreover, the iron peak was visible using both EOs; this is probably owing to the presence of a conservative layer, which can only stiffen the material's surface.

4. Conclusions

GC-MSMS was used to analyze essential oils extracted from the aerial parts of *Artemisia herba-alba* and *Juniperus phoenicea*. Notably, 32 potentially active compounds were identified in *Artemisia herba-alba*, with beta thujone (30.07%) and alpha thujone (13.32%) as the main components, while for *Juniperus phoenicea*, 30 constituents were identified, with alpha-pinene (43.61%) and manoyl oxide (11.50%) as the main components. The results obtained showed that the studied EOs have considerable activity.

In this study, the experimental results were confirmed theoretically using a DFT study after evaluating the inhibition efficiency of two EOs, *Juniperus phoenicea* and *Artemisia herba-alba*. The study conducted on mechanisms of inhibitors revealed several important conclusions. Firstly, the tested essential oils (EOs) were found to be effective inhibitors of mild steel corrosion in 1 M hydrochloric acid, with an inhibitor efficiency reaching 92% at a concentration of 1 g/L. This indicates that the main molecules of the EOs strongly adsorb onto the surface of the mild steel in the acid solution. Secondly, based on the polarization data, the EOs were classified as mixed-type inhibitors, indicating their ability to inhibit both the anodic and cathodic reactions involved in the corrosion process. Thirdly, the use of inhibitors significantly increased the charge transfer values and reduced the double-layer capacity, as revealed by the electrochemical impedance spectroscopy (EIS) results. Furthermore, surface analysis confirmed the formation of a protective film resulting from the adsorption of the studied inhibitors on the mild steel surface. Additionally, density functional theory (DFT) calculations demonstrated that both EOs acted as electron donors/acceptors to and from the iron surface.

Our work meets the approach of the new program of sustainable development in Morocco, whose main vector is green chemistry that reduces and eliminates the use or generation of substances harmful to the environment.

Author Contributions: G.B., M.B. (Mustapha Beniken), R.S., N.A., E.E.-c., Z.R.: writing the original draft, formal analysis, investigation. A.S., H.-A.N., Y.A.B.J., M.B. (Mohammed Bourhia) reviewing and editing, data curation, and funding acquisition. M.T.: supervision. All authors have read and agreed to the published version of the manuscript.

Funding: This work is financially supported by the Researchers Supporting Project (RSP2023R457). King Saud University, Riyadh, Saudi Arabia.

Data Availability Statement: Not applicable.

Acknowledgments: The authors would like to extend their sincere appreciation to the Researchers Supporting Project, King Saud University, Riyadh, Saudi Arabia, for funding this work through project number (RSP2023R457).

Conflicts of Interest: The authors declare that there is no conflict of interest.

References

1. Lahsissene, H.; Kahouadji, A. Analyse ethnobotanique des plantes médicinales et aromatiques de la flore marocaine: Cas de la région de Zaër. *Phytothérapie* **2010**, *8*, 202–209. [[CrossRef](#)]
2. Aimad, A.; Sanae, R.; Anas, F.; Abdelfattah, E.M.; Bourhia, M.; Mohammad Salamatullah, A.; Alzahrani, A.; Alyahya, H.K.; Albadr, N.A.; Abdelkrim, A.; et al. Chemical Characterization and Antioxidant, Antimicrobial, and Insecticidal Properties of Essential Oil from *Mentha pulegium* L. *Evid.-Based Complement. Altern. Med.* **2021**, *2021*, e1108133. [[CrossRef](#)]
3. Boudjouref, M.; Zerrouk, M.M.; Sétif, U.F.A. Etude de L'activité Antioxydante et Antimicrobienne D'extraits D'*artemisiacampestres* L. Master's Thesis, Université Ferhat Abbes, Sétif, Algeria, 2011.
4. Revie, R.W. *Corrosion and Corrosion Control: An Introduction to Corrosion Science and Engineering*, 4th ed.; John Wiley & Sons: Hoboken, NJ, USA, 2008.
5. Shreir, L.L.; Burstein, G.T.; Jarman, R.A. *Corrosion*, 3rd ed.; Butterworth-Heinemann: Oxford, UK; Boston, MA, USA, 1994.

6. Sastri, V.S. *Corrosion Inhibitors: Principles and Applications*; John Wiley & Sons: New York, NY, USA, 1998.
7. Bouyanzer, A.; Hammouti, B. Naturally occurring ginger as corrosion inhibitor for steel in molar hydrochloric acid at 353 K. *Bull. Electrochem.* **2004**, *20*, 63–65.
8. Hammouti, B.; Kertit, S.; Melhaoui, A. Electrochemical behavior of bgugaine as a corrosion inhibitor of iron in 1 M HCl. *Bull. Electrochem.* **1997**, *13*, 97–98.
9. Akrou, A. Etude des huiles essentielles de quelques plantes pastorales de la région de Matmata (Tunisie). *Cah. Options Méditerranéennes* **2004**, *62*, 289–292.
10. Bora, K.S.; Sharma, A. The genus *Artemisia*: A comprehensive review. *Pharm. Biol.* **2011**, *49*, 101–109. [[CrossRef](#)]
11. Ahuja, A.; Yi, Y.-S.; Kim, M.-Y.; Cho, J.Y. Ethnopharmacological properties of *Artemisia asiatica*: A comprehensive review. *J. Ethnopharmacol.* **2018**, *220*, 117–128. [[CrossRef](#)]
12. Benabid, A. *Flore et Écosystèmes du Maroc: Evaluation et Préservation de la Biodiversité*; Librairie et éditions Kalila Wa Dimna: Casablanca, Morocco, 2000.
13. Fennane, M.; Ibn-Tattou, M. *Flore Pratique du Maroc. Vol. 2. Angiospermae (Leguminosae-Lentibulariaceae)*; Inst. Scientifique, Université Mohammed V-Agdal: Rabat, Morocco, 2007.
14. Avato, P.; Laquale, S.; Argentieri, M.P.; Lamiri, A.; Radicci, V.; D'Addabbo, T. Nematicidal activity of essential oils from aromatic plants of Morocco. *J. Pest Sci.* **2017**, *90*, 711–722. [[CrossRef](#)]
15. Meloni, M.; Perini, D.; Filigheddu, R.; Binelli, G. Genetic variation in five Mediterranean populations of *Juniperus phoenicea* as revealed by inter-simple sequence repeat (ISSR) markers. *Ann. Bot.* **2006**, *97*, 299–304. [[CrossRef](#)]
16. Nedjimi, B.; Beladel, B.; Guit, B. Multi-element determination in medicinal Juniper tree (*Juniperus phoenicea*) by instrumental neutron activation analysis. *J. Radiat. Res. Appl. Sci.* **2015**, *8*, 243–246. [[CrossRef](#)]
17. Le Floc'h, E. *Contribution à Une étude Ethnobotanique de la Flore Tunisienne*; Ministère de l'Enseignement Supérieur et de la Recherche Scientifique: Tunis, Tunisia, 1983.
18. Adams, R.P. *Identification of Essential Oil Components by Gas Chromatography/Mass Spectrometry*, 4th ed.; Carol Stream, Allured Pub. Corp.: Illinois, IL, USA, 2007.
19. Arrousse, N.; Mabrouk, E.H.; IsmailiAlaoui, K.; El Hajjaji, F.; Rais, Z.; Taleb, M. Economical synthesis strategy, characterization and theoretical study of the organic dye 3-oxo-3H-spiro [isobenzofuran-1, 9'-xanthene]-3', 6'-diyl dibenzoate. *SN Appl. Sci.* **2020**, *2*, 1019. [[CrossRef](#)]
20. Abdellaoui, O.; Skalli, M.K.; Haoudi, A.; Rodi, Y.K.; Arrousse, N.; Taleb, M.; Ghibate, R.; Senhaji, O. Study of the inhibition of corrosion of mild steel in a 1 M HCl solution by a new quaternary ammonium surfactant. *Moroc. J. Chem.* **2021**, *9*, 44–56.
21. Alaoui Mrani, S.; Ech-chihbi, E.; Arrousse, N.; Rais, Z.; El Hajjaji, F.; El Abiad, C.; Radi, S.; Mabrouki, J.; Taleb, M.; Jodeh, S. DFT and Electrochemical Investigations on the Corrosion Inhibition of Mild Steel by Novel Schiff's Base Derivatives in 1 M HCl Solution. *Arab. J. Sci. Eng.* **2021**, *46*, 5691–5707. [[CrossRef](#)]
22. Arrousse, N.; Mabrouk, E.; Hammouti, B.; El Hajjaji, F.; Rais, Z.; Taleb, M. Synthesis, characterization, anti-corrosion behavior and theoretical study of the new organic dye: 3-oxo-3H-spiro [isobenzofuran-1,9-xanthene]-3,6-diyl bis (3-methyl-benzenesulfonate). *Int. J. Corros. Scale Inhib.* **2020**, *9*, 661–687.
23. Hudaib, M.M.; Aburjai, T.A. Composition of the essential oil from *Artemisia herba-alba* grown in Jordan. *J. Essent. Oil Res.* **2006**, *18*, 301–304. [[CrossRef](#)]
24. Zaim, A.; El Ghadroui, L.; Farah, A. Effets des huiles essentielles d'*Artemisia herba-alba* sur la survie des criquets adultes d'*Euchorthippus alboblineatus* (Lucas, 1849). *Bull. L'institut Sci. Rabat Sect. Sci. Vie* **2012**, *34*, 127–133.
25. Ghanmi, M.; Satrani, B.; Aafi, A.; Isamili, M.R.; Houti, H.; El Monfalouti, H.; Benchakroun, K.H.; Aberchane, M.; Harki, L.; Boukir, A.; et al. Effet de la date de récolte sur le rendement, la composition chimique et la bioactivité des huiles essentielles de l'armoise blanche (*Artemisia herba-alba*) de la région de Guerçif (Maroc oriental). *Phytothérapie* **2010**, *8*, 295–301. [[CrossRef](#)]
26. Bezza, L.; Mannarino, A.; Fattarsi, K.; Mikail, C.; Abou, L.; Hadji-Minaglou, F.; Kaloustian, J. Chemical composition of the essential oil of *Artemisia herba-alba* issued from the district of Biskra (Algeria). *Phytothérapie* **2010**, *8*, 277. [[CrossRef](#)]
27. Dob, T.; Benabdelkader, T. Chemical composition of the essential oil of *Artemisia herba-alba* Asso grown in Algeria. *J. Essent. Oil Res.* **2006**, *18*, 685–690. [[CrossRef](#)]
28. Dhifallah, A.; Rouissi, H.; Selmi, H. Evaluation of the antioxidant and antibacterial activities of Tunisian *Artemisia herba-alba* essential oil. *Moroc. J. Agric. Sci.* **2021**, *2*, 114–117.
29. Elmhalli, F.; Garbou, S.S.; Karlson, A.K.B.; Mozūraitis, R.; Baldauf, S.L.; Grandi, G. Acaricidal activity against *Ixodes ricinus* nymphs of essential oils from the Libyan plants *Artemisia herba alba*, *Origanum majorana* and *Juniperus phoenicea*. *Vet. Parasitol. Reg. Stud. Rep.* **2021**, *24*, 100575.
30. Boumhara, K.; Harhar, H.; Tabyaoui, M.; Bellaouchou, A.; Guenbour, A.; Zarrouk, A. Corrosion inhibition of mild steel in 0.5 M H₂SO₄ solution by *Artemisia herba-alba* oil. *J. Bio-Tribo-Corros.* **2019**, *5*, 8. [[CrossRef](#)]
31. Tilaoui, M.; Ait Mouse, H.; Jaafari, A.; Zyad, A. Comparative phytochemical analysis of essential oils from different biological parts of *Artemisia herba alba* and their cytotoxic effect on cancer cells. *PLoS ONE* **2015**, *10*, e0131799. [[CrossRef](#)]
32. Ennajar, M.; Bouajila, J.; Lebrihi, A.; Abderraba, M.F.; Raies, A.; Romdhane, A. Chemical Composition and Antimicrobial and Antioxidant Activities of Essential Oils and Various Extracts of *Juniperus phoenicea* L. (Cupressaceae). *J. Food Sci.* **2009**, *74*, M364–M371. [[CrossRef](#)]

33. Keskes, H.; Mnafigui, K.; Hamden, K.; Damak, M.; El Feki, A.; Allouche, N. In vitro anti-diabetic, anti-obesity and antioxidant proprieties of *Juniperus phoenicea* L. leaves from Tunisia. *Asian Pac. J. Trop. Biomed.* **2014**, *4*, S649–S655. [[CrossRef](#)]
34. Aafi, A.; Taleb, M.S.; Fechtal, M. *Espèces Remarquables de la Flore du Maroc*; CNRF: Mechanicsville, VA, USA, 2002; Volume 146.
35. Ait-Ouazzou, A.; Lorán, S.; Arakrak, A.; Laglaoui, A.; Rota, C.; Herrera, A.; Pagán, R.; Conchello, P. Evaluation of the chemical composition and antimicrobial activity of *Mentha pulegium*, *Juniperus phoenicea*, and *Cyperus longus* essential oils from Morocco. *Food Res. Int.* **2012**, *45*, 313–319. [[CrossRef](#)]
36. Bahri, F.; Romane, A.; Arjouni, Y.; Harrak, R.; Ahmed El Alaoui El Fels, M. Chemical composition and antibacterial activity of the essential oil of Moroccan *Juniperus phoenicea*. *Nat. Prod. Commun.* **2011**, *6*, 1515–1518.
37. Bouzouita, N.; Kachouri, F.; Ben Halima, M.; Chaabouni, M.M. Composition chimique et activités antioxydante, antimicrobienne et insecticide de l'huile essentielle de *Juniperus phoenicea*. *J. Soc. Chim. Tunis* **2008**, *10*, 119–125.
38. El-Sawi, S.; Motawae, H.; Ali, M. Chemical composition, cytotoxic activity and antimicrobial activity of essential oils of leaves and berries of *Juniperus phoenicea* grown in Egypt. *Afr. J. Tradit. Complement. Altern. Med.* **2007**, *4*, 417. [[CrossRef](#)] [[PubMed](#)]
39. Adams, R.P.; Barrero, A.F.; Lara, A. Comparisons of the leaf essential oils of *Juniperus phoenicea*, *J. phoenicea* subsp. *eu-mediterranea* Lebr. & Thiv. and *J. phoenicea* var. *turbinata* (Guss.) Parl. *J. Essent. Oil Res.* **1996**, *8*, 367–371.
40. Ghouti, D.; Rached, W.; Abdallah, M.; Pires, T.C.; Calhelha, R.C.; Alves, M.J.; Abderrahmane, L.H.; Barros, L.; Ferreira, I.C. Phenolic profile and in vitro bioactive potential of Saharan *Juniperus phoenicea* L. and *Cotula cinerea* (Del) growing in Algeria. *Food Funct.* **2018**, *9*, 4664–4672. [[CrossRef](#)] [[PubMed](#)]
41. Achak, N.; Romane, A.; Abbad, A.; Ennajar, M.; Romdhane, M.; Abderrabba, A. Essential oil composition of *Juniperus phoenicea* from Morocco and Tunisia. *J. Essent. Oil Bear. Plants* **2008**, *11*, 137–142. [[CrossRef](#)]
42. Fernine, Y.; Ech-chihbi, E.; Arrousse, N.; El Hajjaji, F.; Bousraf, F.; Touhami, M.E.; Rais, Z.; Taleb, M. *Ocimum basilicum* seeds extract as an environmentally friendly antioxidant and corrosion inhibitor for aluminium alloy 2024-T3 corrosion in 3 wt% NaCl medium. *Colloids Surf. A Physicochem. Eng. Asp.* **2021**, *627*, 127232. [[CrossRef](#)]
43. Abdelahi, M.M.; Elmsellem, H.; Benchidmi, M.; Sebbar, N.K.; Belghiti, M.A.; El Ouasif, L.; Jilalat, A.E.; Kadmi, Y.; Essassi, E.M. A DFT and molecular dynamics study on inhibitory action of indazole derivative on corrosion of mild steel. *J. Mater. Environ. Sci.* **2017**, *8*, 1860–1876.
44. Zaidi, S.Z.J.; Hassan, S.; Raza, M.; Walsh, F.C. Transition metal oxide as possible electrode materials for Li-ion batteries: A DFT Analysis. *Int. J. Electrochem. Sci.* **2021**, *16*, 210322. [[CrossRef](#)]
45. Mrani, S.A.; Arrousse, N.; Haldhar, R.; Lahcen, A.A.; Amine, A.; Saffaj, T.; Kim, S.-C.; Taleb, M. In Silico Approaches for Some Sulfa Drugs as Eco-Friendly Corrosion Inhibitors of Iron in Aqueous Medium. *Lubricants* **2022**, *10*, 43. [[CrossRef](#)]
46. Obot, I.B.; Haruna, K.; Saleh, T.A. Atomistic Simulation: A Unique and Powerful Computational Tool for Corrosion Inhibition Research. *Arab. J. Sci. Eng.* **2019**, *44*, 1–32. [[CrossRef](#)]
47. Ricky, E.X.; Mpelwa, M.; Xu, X. The study of m-pentadecylphenol on the inhibition of mild steel corrosion in 1 M HCl solution. *J. Ind. Eng. Chem.* **2021**, *101*, 359–371. [[CrossRef](#)]
48. Goyal, M.; Kumar, S.; Bahadur, I.; Verma, C.; Ebenso, E.E. Organic corrosion inhibitors for industrial cleaning of ferrous and non-ferrous metals in acidic solutions: A review. *J. Mol. Liq.* **2018**, *256*, 565–573. [[CrossRef](#)]
49. Galai, M.; Rbaa, M.; Ouakki, M.; Dahmani, K.; Kaya, S.; Arrousse, N.; Dkhireche, N.; Briche, S.; Lakhrissi, B.; Touhami, M.E. Functionalization effect on the corrosion inhibition of novel eco-friendly compounds based on 8-hydroxyquinoline derivatives: Experimental, theoretical, and surface treatment. *Chem. Phys. Lett.* **2021**, *776*, 138700. [[CrossRef](#)]
50. Ayuba, A.M.; Abubakar, M. A Theoretical Study on Isolated Compounds from the Leaves Extract of *Guiera Senegalensis* as Aluminium Corrosion Inhibitor. *J. Sci. Technol.* **2021**, *13*, 47–56.
51. Chile, N.E.; Haldhar, R.; Godffrey, U.K.; Chijioke, O.C.; Umezuruike, E.A.; Ifeoma, O.P.; Oke, M.O.; Ichou, H.; Arrousse, N.; Kim, S.-C.; et al. Theoretical Study and Adsorption Behavior of Urea on Mild Steel in Automotive Gas oil (AGO) Medium. *Lubricants* **2022**, *10*, 157. [[CrossRef](#)]

Disclaimer/Publisher's Note: The statements, opinions and data contained in all publications are solely those of the individual author(s) and contributor(s) and not of MDPI and/or the editor(s). MDPI and/or the editor(s) disclaim responsibility for any injury to people or property resulting from any ideas, methods, instructions or products referred to in the content.